Author version: Marine Geology: 247(3-4); 2008; 178-193

Possible detrital, diagenetic and hydrothermal sources for Holocene sediments of the Andaman backarc basin

Siby Kurian, B. Nagender Nath [1], V. Ramaswamy, D. Naman, T. Gnaneshwar Rao*, K.A. Kamesh Raju, K. Selvaraj, C.T.A. Chen****

National Institute of Oceanography, Dona Paula, Goa-403 004, India

*National Geophysical Research Institute, Uppal Road, Hyderabad-500 007, India

** Institute of Marine Geology & Chemistry, National Sun Yat-Sen University, Kaohsiung 804, Taiwan

[1] Corresponding author, E-mail: nagender@nio.org

Phone: 91-832 2450402

Fax: 91-832-2450609

Abstract

Three sediment cores near the spreading axis in the Andaman backarc basin (ABB) were studied for bulk and clay mineralogy, major, trace and rare earth element (REE) geochemistry in bulk and three selective leaches, to identify sediment sources to this region and to decipher probable hydrothermal contribution. REE and other geochemical data suggest a strong influence of the Irrawaddy River as a major continental source to the ABB sediments. Low carbonate content in the sediments is due to dilution by higher detrital input as well as reduced foraminiferal carbonate contribution because of low sea surface salinity. The contribution from local volcanic sources was identified from the presence of volcanic glass in the sand-sized sediment fraction; higher smectite content in the clay fraction and the trace element data. Mn concentrations in the upper 12 cm are well above those found in pelagic carbonate-free sediments. Mn distribution pattern and oxide nature suggest a hydrothermal source. Other discriminants such as Eu anomaly and Y/Ho ratio also suggest the role of hydrothermal activity. In addition, the association of Mo with Pb, Zn and Cu in the HCl–insoluble residue suggests the presence of sulfidic material probably of hydrothermal origin.

Keywords: Andaman backarc basin, Irrawaddy River, rare earth elements, geochemical tracers, volcanic sources, hydrothermal mineralization

1. Introduction

The tectonics and geological history of the Andaman Sea is fairly well known (Rodolfo, 1969; Curray et al., 1979; Rao et al., 1996; Kamesh Raju et al., 2004), but limited studies have been carried out on the sediments (Cronan and Wijayananda, 1991; Roonwal et al., 1997; Venkatesan et al., 2003). According to Rodolfo (1969), the main sources of sediments to the Andaman basin are the Irrawaddy, Salween and Sittang Rivers from Myanmar. Recent studies (Ramaswamy et al., 2004; Rao et al., 2005) have shown that the sediment influx from these rivers is transported along the shelf by monsoon currents and carried to the deep sea floor through submarine canyons.

Apart from fluvial sources (Roonwal et al., 1997), the ABB should also receive material from pelagic, eolian, weathering of sea-floor rocks, and possible hydrothermal sources (Rao et al., 1996; Chernova et al., 2001; Venkatesan et al., 2003; Siby, 2004). Assessing the sources to the ABB assumes importance in view of the following:

1) Rodolfo (1969) reported high smectite content for the deep Andaman sea sediments, though the main fluvial source of sediments to the region has low smectite content (Konta, 1985).
2) Paleoclimatic reconstructions on the sediments of ABB were conducted (e.g. Colin et al., 1999) on the assumption that the main source of sediments to the Andaman Sea is the Irrawaddy River. However, other sources are likely to play a role in the basinal sedimentation in view of its tectonic setting.
3) Backarc basins are known for hydrothermal mineralization (e.g. Sumisu Rift, Izu Bonin Island Arc, Okinawa Trough, Mariana Trough, Mariana Basin,

Manus Basin, North Fiji Basin, Lau Basin etc. (Rona and Scott, 1993 and references therein)). The ABB has a well defined spreading axis (Kamesh Raju et al., 2004) and the possibility of hydrothermal signatures in the basin is reported by Rao et al., (1996). So, it is interesting to see if any hydrothermal signatures are seen in the ABB sediments.

With the above objectives, we have studied 3 short sediment cores collected on either side of the rift valley in the ABB for 1) mineralogy of clay-sized fraction and bulk sediments; 2) comprehensive geochemical studies on a) whole-sediments and b) on three chemically separable phases (both leach and residue), extracted using selective leaching techniques.

2. Materials and methods

2.1 Study area

The ABB is a semi-enclosed basin in the eastern Indian Ocean. The basin is marked by prominent morphological features such as the Nicobar deep, Barren-Narcondam volcanic islands, Invisible bank and Alcock and Sewell seamount complexes (Rodolfo, 1969a). The southwestern part of the basin is dominated by N-S-trending fault systems. The backarc basin is bisected by a prominent trough (with a vertical drop of about 500m), which makes the Andaman backarc spreading center (Kamesh Raju et al., 2004). The western part is dominated by volcanic features which are related to arc volcanism and backarc spreading activity, whereas the eastern part has a smooth topography resulting from sediment infill from the Irrawaddy and Salween River system located to the north of the study area (Fig.1).

The Andaman Sea experiences the seasonally reversing Asian monsoon (Wyrtki, 1973). Circulation in the Andaman Sea is cyclonic during the southwest monsoon (May-September) and anti-cyclonic during the northeast monsoon (December-February). Surface salinities are variable owing to intermittent dilution by monsoonal precipitation and runoff from the Irrawaddy and Peninsular Myanmar. This results in low surface salinity (<30 PSU) in the northern area, which increases southwards to more normal marine values (Rodolfo, 1969). The surface seawater temperatures are quite uniform throughout the year, ranging between 27° and 30° C.

2.2 Sample Collection

In the present study, three short spade cores SPC-1 (11.17°N, 94.73°E), SPC-2 (10.58°N, 94.72°E) and SPC-5 (10.31°N, 94.39°E) [~20 - 30 cm long] were collected during the 168th expedition of O.R.V. Sagar Kanya in 2001. They were sub-sampled at 2 cm intervals and divided into two aliquots. One aliquot was frozen for geochemical studies, while the second half was dried at 65°C for sedimentological analyses. Based on a sedimentation rate of ~10 cm kyr^{-1} in the basin (Colin et al., 1999; Ahmad et al., 2000 and the unpublished data with the authors), the sediments sampled are not older than ~3 kyr. While the core SPC-1 was sampled from the northern side of the rift valley, SPC-2 and SPC-5 were collected from the southern side of the rift valley (Fig. 1). Three surface sediment samples and suspended sediment from the inner continental shelf were also analyzed to represent the fluvial contribution from Irrawaddy and Salween Rivers (Fig. 1).

2.3 Mineralogy

Observations under binocular microscope show that the coarse fraction (>63 μm) is a mixture of biogenic particles such as radiolarians and foraminifera, with ferromanganese micronodules noticed in a few samples. Small quantities of palagonitic material, muscovite, biotite and glass fragments (brown and white colored) were also observed at deeper sediment intervals.

2.3.1 Bulk mineralogy: Sediment samples were washed until salt free, treated with H_2O_2 to remove organic carbon and freeze dried for bulk mineralogical analysis. Homogenised sediment samples were pressed into sample holders taking care to minimize orientation of the particles. Samples were scanned from 3° to 32° 2θ at 0.5° 2θ min^{-1} on a X- ray Diffractometer using Cu Kα radiation. The percentages of various minerals were determined following the method of Biscaye (1965).

2.3.2 Clay mineralogy: Sediment fractions <2μm were separated for clay mineral analysis based on the settling velocity (Folk, 1968). Salt and organic carbon- free clay fractions were prepared as a thick slurry, pipetted onto glass slides, glycolated overnight at 60°C and kept in the desiccator. The slides were scanned from 3° to 32° at 2° 2θmin^{-1} with slow speed (24° to 26° at 0.01° 2θ sec^{-1}) on X- ray Diffractometer using Cu Kα radiation. The relative abundance of the clay minerals was determined according to the method described in Biscaye (1965) using weighted peak areas (4 x illite, 2 x (kaolinite and chlorite) and 3.33 x quartz). For Identification of smectite types, sediment samples <2 μm fraction were freeze dried, homogenized and pressed into holders (less oriented) and were scanned from 48° to 64° 2θ on the X- ray diffractometer using Cu Kα

radiation. This scanning range includes smectite (060) at 1.501-1.503°A, quartz peak (112) at 1.817°A and quartz peak (211) at 1.524°A +/- 0.001°A.

2.4 Bulk Geochemistry

In the laboratory, the dried samples were grinded to fine powder using an agate mortar and pestle. The calcium carbonate content was measured using a CO_2 Coulometer following acidification of the sample with 1N HCl. The organic carbon (C_{org}) content was determined by the wet oxidation method (El Wakeel and Riley, 1957). The precision and accuracy of the analysis were better than 0.01% and 7-10% respectively (Nath et al., 1997). Analysis for REEs and other trace elements were carried out at NGRI, Hyderabad, using an ICP-MS. Sediments and geochemical standard (MAG-1 from the USGS) were dissolved following acid dissolution procedure described in Balaram and Rao (2003). Potential polyatomic and doubly charged ion interferences were minimized by choosing the least interfering isotopes of each element as well as by diluting the solutions considerably (5000 times). The results showed better than 1% agreement for the REEs with respect to MAG-1. Co, Ni, Cu, La, Nd, Er analyses had a precision of 1%, while all other elements has displayed precisions better than 5%. The error calculated in the Eu anomaly is <0.02 anomaly unit, hence the Eu anomaly has been considered in the discussion only if the variation between samples exceeds this value.

Ba and K were analyzed in two cores (SPC-1 and SPC-5) using an X-ray fluorescence spectrometer (RIGAKU RIX 2000) equipped with a Rh cathode. About 2 g of finely powdered (<200 mesh) sediment with silica gel 60 (Merck) added as binder and compacted into pellets (30 mm in diameter and 10 mm thick) under 20 x 10^3 Kg cm^{-2}

pressures. The pellets were analyzed at an acceleration voltage of 50kV and a current of 50 mA. The accuracy of the analytical method, determined by analyzing the standard reference materials (GBW 07315 and GBW 07316 [marine sediments]), was better than 3%.

2.5 Leach studies

Selective leach studies were carried out following the method described by Cronan (1976). Three splits of 1g sediment were leached separately using 1) 10% acetic acid, 2) mixed acid-reducing agent (acetic acid and hydroxylamine-HCl) and 3) with hot 50% HCl. The leach solutions and residues were analyzed for REEs and other elements by means of ICP-MS. Using the three selective leaches (L1, L2 and L3), the following element associations were established. (1) Acetic acid (L1) dissolves carbonate mineral constituents, loosely sorbed ions, and interstitial water evaporates and possibly some colloidal iron. (2) The acid reducing agent (L2) removes all the above phases together with ferromanganese oxide and some amorphous Fe-oxides. (3) Hot HCl (L3) removes phase 1, phase 2, along with bulk of remaining amorphous Fe-oxide, crystalline Fe-oxide and partially dissolves clays and other weathered detrital phases. 4) Any material not dissolved by the HCl consists of resistant silicates and aluminosilicates (Cronan, 1976; Hodkinson et al., 1994). The elements (wt %) soluble in each phase such as acetic acid soluble (L1), hydroxylamine-HCl soluble (L2-L1), HCl soluble (L3-L2) and detrital fraction (HCl insoluble fraction) were calculated from these results.

3. Results

3.1 Mineralogy

The down core variations of bulk minerals (quartz and plagioclase) and clay minerals (smectite, illite, chlorite and kaolinite) from the ABB are listed in Table 1. The quartz concentration increased down core for SPC-1 sediments, while those from SPC-2 decreased. Plagioclase ranged between 6 to 11% for all the samples with low values in the deeper sample intervals. The major clay minerals present are smectite (34-60%), Illite (19-35%), kaolinite (7-16%) and chlorite (6-12%) (Table1). The illite concentration ranged between 20- 35% for SPC-1 and SPC-5 with high values corresponding to a low smectite abundance. Kaolinite abundance was higher than that of chlorite with an average K/Ch ratio of 1.3 (Table 1). The Smectite type was identified as dioctahedral montmorillonite and beidellite based on d (060) spacing (1.501-1.503°A). The beidellite could be either Al-beidellite or Al-Fe beidellite (Parra et al., 1991).

3.2 Bulk Geochemistry

The $CaCO_3$ content is low for the surface samples of all the three cores ranging from 0.3 - 2.8 (wt %), and increased to 8 (wt%) for the deeper sediment intervals (SPC-1 and SPC-5) and to 18 (wt%) for SPC-2 (Table 2). The organic carbon content in the surface sediments of SPC-1 was low (0.44%), but varied between 1.26-1.96% for all other samples from the ABB (Table 2). The concentrations of a few important major, trace elements and REEs for sediments from the ABB and Irrawaddy shelf are presented in Tables 2 and 3. The Al concentrations did not show much variation (8- 9%) for the samples from the ABB and Irrawaddy shelf. Fe concentration ranged between 4.3 to 5% for SPC-1 and SPC-5 sediments, but a relatively low concentration (3.6 - 4.6%) was recorded in SPC-2 and a high concentration in sediments from Irrawaddy

shelf (6- 6.3%). K concentration ranged between 1.8- 2.04 % for SPC-1 and SPC-5 sediments with low concentration for the surficial samples. Elements such as Mn, Ba, Co, Ni, Cu displayed low concentration in the deeper sediment intervals (Table 2). Mn showed high concentration (1 to 4%) in the top 6 cm after which they rapidly decreased and reached uniformly low concentration (<0.4%) in the deeper sample intervals. Similar high values are also noted for Mo (Table 2).

The REEs are normalized to Post Archaean Australian Shale (PAAS) concentrations taken from Taylor and McLennan (1985) and the shale-normalized patterns are shown in Figure 2. SPC-1 and SPC-5 showed higher total REE concentrations (ΣREE) for the deeper samples (Fig. 3a). Shale normalized patterns (Fig.2) are nearly flat except positive Eu anomalies for all the cores (1.1 to 1.28). The Ce anomaly is not significant in these samples (Table 3), while the Eu anomaly decreases gradually with increasing sediment depth (Fig. 3b). Shale-normalized La/Yb ratios showed low values for surface samples (0.85) which increase towards the base of the core (1.23) (Table 3). The variation is more marked for core SPC-1.

3.3 Leach studies

The weight percent of elements soluble in each phase viz. 1) acetic acid; 2) hydroxylamine-HCl; 3) soluble in HCl; and 4) HCl insoluble residue (detrital fraction) are shown in Table 4. About 13-28% of sediment fraction was leached out by acetic acid (biogenic fraction), 18-32% in hydroxylamine-HCl and 30-46% in HCl. Resistant detrital and volcaniclastic phases contribute to 60-70% in the HCl insoluble residue (Table 4).

Mn showed high percentage in the hydroxylamine-HCl soluble phase (ferromanganese oxide) with high values for the surface samples. Elements like Fe, Cr, Co, Ni, Cu, Zn showed higher percentage in the HCl soluble fraction indicating that

these elements are more associated with crystalline Fe-oxides. The high field strength elements such as Ga, Nb, Th. are more associated with detrital fraction (HCl insoluble residue is about 65-95%), while their contribution to other phases is negligible (Table 4). The total REE content (ΣREE) showed a low percentage in acetic acid fraction for all the three cores with relatively high values for the deeper sample intervals. The contribution of ΣREE to the HCl soluble fraction is 30-40%. Shale-normalized patterns of acetic acid soluble phase (biogenic carbonates) in the surface sediments showed HREE enrichment and negative Ce anomaly (Fig. 4) mimicking the seawater REE pattern (Palmer, 1985; Chavagnac et al., 2005). The deeper samples showed flat or insignificant positive Ce anomaly.

4. Discussion

4.1 Source of Andaman backarc basin sediments

Deciphering the provenance of hemipelagic sediments is complicated owing to their fine-grained nature of the sediment and the multiple processes of transport and resuspension controlling their distribution (e.g. Hathon and Underwood, 1991; Stow, 1985). In addition, the Andaman basin also receives sediment inputs directly from the Myanmar shelf through the Martaban canyon (Ramaswamy et al., 2004; Rao et al., 2005). Seismic studies show that the Irrawaddy River as the major source of detrital sediment in the abyssal plain in the eastern part of the ABB (Kamesh Raju et al., 2004).

4.1.1. Terrigenous source:

The similarity in shale-normalized REE patterns with positive Eu anomaly for sediments from both the ABB and the Irrawaddy shelf (Fig 2) suggest that the Myanmar

Rivers are the major continental source to the ABB sediments (Roonwal et al., 1997). Flat shale-normalized patterns for the ABB and Irrawaddy shelf sediments indicate a mixed felsic and basic source (Piper, 1974; Sholkovitz, 1990; McLennan, 1989; Nath et al., 2000). However, there are dissimilarities in the patterns between the ABB and Irrawaddy shelf sediments (Fig. 2) which are discussed in the subsequent sections. The fractionation index $(La/Yb)_n$ [Table 3] shows high values for the deeper samples (typical of continentally-derived detrital material) which suggest a larger detrital component in the older sediments (Piper, 1974; Sholkovitz, 1990; Nath et al., 1997).

4.1.2. Biogenic source:

Although the organic carbon content in the core tops (0.44 to 1.82%; Table 2) is within the range expected of hemi-pelagic sediments, the $CaCO_3$ content is very low (0.5 to 2.8 wt %). It is surprising to find such a low carbonate content in a modern hemipelagic sedimentation area at a depth of 3000 m. In a similar setting and water depth in the Arabian Sea, carbonate percentages are around 30-40% (e.g., Sirocko et al., 2000). The extremely low carbonate content in the surface of the core tops from the ABB are both due to the dilution from large detrital sedimentation and the lower foraminiferal carbonate productivity induced by sharp changes in surface salinity (<30 PSU) during the southwest monsoon in the northern Bay of Bengal and Andaman Sea (Ramaswamy and Gaye, 2006; Stoll et al., 2007). Contributions from the Irrawaddy shelf is mainly fluvial sediment having low carbonate content (<1%, Table 2).

4.1.3. Volcanic source:

Tephra present in the sand-sized sediment fractions from the ABB sediments indicates contribution from arc volcanism and numerous seamounts in the western backarac basin (Rao et al., 1996; Kamesh Raju et al., 2004). Although the shale-normalized patterns of the sediments from the ABB and Irrawaddy shelf are broadly similar, the relative LREE depletion in the ABB sediment (Fig. 2) suggests a possible contribution from local basaltic sources. The higher smectite content (~50%) in the clay fraction of ABB sediment compared to that of Irrawaddy shelf sediment (15%) also supports the contribution from volcanic rocks (Fig 5).

The smectite in ABB sediments is identified as dioctahedral montmorillonite and beidellite. The occurrence of Al-smectite in the sediments could indicate the presence of terrigenous smectite (Aoki and Kohyama, 1991; Chamley, 1989) or smectite derived from the hydrothermal alteration of volcanic formation and soils (Parra et al., 1991). The higher smectite content in the clay fraction of ABB sediments compared to Irrawaddy source could therefore indicate mixed sources of continental, volcanic and hydrothermal smectite. Alternatively, smectite usually the clay mineral having the smallest particles could be transported furthest away from the Irrawaddy River, increasing its relative concentration in the deep ABB sediments.

Basaltic rocks were recovered from the ABB spreading centre and flanks of the rift valley by Rodolfo (1969), Rao et al., (1996) and Curray, (2005). The compositional data also supports a basaltic contribution to the sediments for e.g. Sc concentrations in residue 3 are closer to the basaltic field (Table 4).

4.2. Hydrothermal signatures:

While the mineralogical and geochemical signatures clearly suggest the contribution from Irrawaddy and other Myanmar Rivers and local basaltic sources, some of the geochemical data requires additional diagenetic and hydrothermal inputs to explain the variations. The following discussions are to differentiate between the diagenetic and hydrothermal signatures, for which we have used Mn, Ba, Mo enrichment, Eu anomaly, Y/Ho variation and Irrawaddy normalized HCl insoluble residue.

(i) *4.2.1. Enrichment of Mn, Ba and Mo:*

The possible sources of Mn enrichment at the surface (Fig. 6) could be either diagenetic or hydrothermal. Mn profiles for SPC-1 show significant enrichment (1- 4%) in the top 12 cm (Fig. 6), well above those in normal pelagic carbonate-free sediments (e.g., Rutten and De Lange, 2003). The deeper samples of the cores have very low Mn content and thus can be clay mineral-Mn or carbonate-Mn (Table 4). Leach studies (Table 4) and PAAS normalized REE patterns (Fig.4) confirm that Mn in the surficial sediments is predominantly in the oxide/oxyhydroxide form. Positive Ce anomalies (1.2 to 1.3) and MREE enrichment (Fig. 4), typical of deep-sea Fe-Mn oxyhydroxides (Elderfield and Greaves, 1981; Glasby et al., 1987; Nath et al., 1992; 1994) are seen here.

Lack of sharp peaks of MnO_2, which is typical of migration of oxidation fronts in a diagenetic system (e.g., Froelich et al., 1979; Thomson et al., 1995; Reitz et al., 2006), suggests that Mn enrichment in the upper sediment zone are not due to diagenetic processes and hydrothermal input play a major role (Reitz et al, 2006).

Barium in the surficial sediments is also high (>1000ppm) up to a depth of 12 cm, which corresponds well with the Mn enriched layers (Table 2, Fig. 6). The enrichment of Ba, Mo and Mn is possible in sediments with hydrothermal/metalliferous components. Hydrothermal sediments, particularly those in proximity to hydrothermal vents may be rich in Ba (Plank and Langmiur, 1998). Although, the barium enrichment can also result from the biological productivity in the overlying waters, a lack of correlation between Ba and other biological proxies ($CaCO_3$, C_{org}) suggests a limited role of productivity on the Ba enrichment in the surficial layers.

Mo enrichment, as high as 200 ppm, is seen in TAG metalliferous sediments (Mills et al., 1993). Similar concomitant increases of Mn and Mo were seen by Schaller et al. (2000) in a sediment core recovered from near an active hydrothermal location on the southern East Pacific Rise and were attributed to the scavenging of dissolved Mo onto Fe and Mn oxides in hydrothermal plumes and diagenetic cycling of Mn in the sediments. The sharp increase in Mo concentrations (from 0.8 to 44 ppm in SPC-1) at the surface in the ABB sediments (Table 2) indicates probable hydrothermal enrichment.

4.2.2. Eu anomaly:

Larger positive Eu anomalies in the ABB sediments (Table 3) compared to the Irrawaddy shelf sediments, could be possibly due to a hydrothermal input. The hydrothermal solutions and the sediments resulting from high-Temparature basalt alteration along the mid-ocean ridges and back-arc spreading centers (Michard et al., 1983; German et al., 1993) display positive Eu anomalies. While the surface sediments

from the ABB showed $(Eu/Sm)_n$ ratios (1.24) closer to hydrothermal plume particle ratio of 1.23 (e.g. Barrett et al., 1990), lower ratios in deeper sediment intervals are more closer to the Irrawaddy shelf sediments (1.1) [Table 3]. This suggests a reduced influence of detrital contribution with time. The larger detrital contribution for the deeper samples is also supported by an increase in down core K content (Table 2). The Eu anomaly, however, can also be a result of eolian input (Elderfield, 1988) or merely due to the variation in plagioclase content. Eolian input to the ABB is not expected as the main-land around the Andaman Sea (Myanmar, Thailand, Andaman islands) is well vegetated and has a humid climate. Hydrothermally-derived metalliferous sediments typically show shale-normalized pattern with HREE enrichment, positive Eu anomaly and negative Ce anomaly similar to seawater (e.g. Bender et al., 1971; Dymond et al., 1973; Mills et al., 1993). However, ABB sediments show a down core decrease in positive Eu anomaly and with no Ce fractionation suggesting that detrital sedimentation in ABB dominates over a hydrothermal contribution.

4.2.3. Y-Ho variation:

Yttrium and the redox-insensitive REEs are very similar, being trivalent with similar ionic radii. These similarities often lead to extremely coherent behavior resulting in negligible Y-Ho fractionation in igneous rocks and clastic sediments (Bau and Dulski, 1999). A plot of Y/Ho (molar ratio) versus Y/Fe x 10^5 (molar ratio) for ABB samples (Fig. 7) shows that the values are close to plume particles from other hydrothermal area indicating affinity to plume characteristics. When we consider the estimates of Y/Ho molar ratio for particles precipitated from varying mixtures of hydrothermal fluids and seawater, the average molar Y/Ho ratios of 57.5, 58.1 and 57.7 obtained for leach-3 of sediments from

the ABB (SPC-1, 2 and 5 respectively) match well with the published values of particles of other areas having ~10% hydrothermal component (Bau and Dulski, 1999).

4.2.4. Concentrations of HCl insoluble fraction normalized to Irrawaddy shelf sediment data:

Normalized to the Irrawaddy sediment, elements such as Mo, Cu, Pb showed enrichment (0.9- 2.4) which is probably due to the hydrothermal input (residue devoid of adsorbed and diagenetic phases). Association of Mo and Cu can be possibly due to sulfide like material, probably of a hydrothermal nature.

Leaching studies reveal a major contribution from resistant detrital and volcaniclastic phases to the ABB sediments (~65%), and thus a mixture of biogenic, authigenic and hydrothermal inputs will account for about 30-40 % (Table 4) in these sediments. The Pb, Zn and Cu content in the present study is 8-10 times lower than in near-vent sediment cores closer to the hydrothermal vents from the EPR area (German et al., 1999). The influence of hydrothermal contribution in the sediments considered here must therefore be limited, compared to other active hydrothermal areas (German et al., 1999) suggesting that these sediments do not represent a near field component derived from erosion and mass wasting of seafloor hydrothermal sulfide deposits but probably represent a weak plume related component (German et al., 1993; Mills et al., 1993).

5. Summary and conclusions

Mineralogical and geochemical studies of the sediments from the ABB show that the principle sediment sources to the basin are (a) the continental source of

Irrawaddy and other Myanmar rivers; (b) biogenic sources; (c) altered products of basinal volcanic rocks which are further subjected to diagenetic and hydrothermal alterations.

High terrigenous and low biogenic carbonate content in the ABB sediment is due to direct input of fluvial sediments through the Irrawaddy sub-marine canyon and low carbonate productivity in the overlying surface waters of the northern Andaman Sea.

Our study indicates a significant enrichment of trace metals (Mn, Ba, Mo, Cu, Pb) in upper 10 cm of the sediment core mainly due to hydrothermal activity. Other hydrothermal signatures such as Eu anomaly, Y/Ho variation, Irrawaddy normalized HCl insoluble residue also support hydrothermal activity during the late Holocene.

Future studies targeting fresh hydrothermal precipitates on basaltic rocks in the rift valley may provide insights into the hydrothermal processes operating in the area.

Acknowledgements

We thank the Directors of NIO, Goa and NGRI, Hyderabad, for permission to use the facilities, the Ministry of Earth Sciences, New Delhi, for providing ship time to collect the samples, CSIR and DST for funding the project, P. Pawaskar, R. Uchil and M. B. L. Mascarenhas-Pereira for their help in generating some of the figures and Girish Prabhu for his help in the XRD analyses. First author wishes to acknowledge Dr. N. Chandramohana Kumar and Dr. K.K.C. Nair for their guidance. K.S. also thanks National Science Council of Taiwan (NSC-94-2621-Z-110-001 and 94-2611-M110-001) for his postdoctoral fellowship. This is NIO contribution No. xxxx

References

Ahmad, S.M., Patil, D.J., Rao, P.S., Nath, B.N., Rao, B.R., Rajagopalan, G., 2000. Glacial-interglacial changes in the surface water characteristics of the Andaman Sea: Evidence from stable isotopic ratios of planktonic foraminifera. Proc. Indian Acad. Sci. (Earth Planet. Sci.) 109, 153-156.

Aoki, S., Kohyama, N., 1991. The vertical change in clay mineral composition and chemical characteristics of smectite in sediment cores from the southern part of the Central Pacific Basin. Mar. Geol. 98, 41-49.

Balaram, V., Rao, T.G., 2003. Rapid determination of REEs and other trace elements in geological samples by microwave acid digestion and ICP-MS. Atomic spectroscopy, 24, 206-212.

Barrett, T.J., Jarvis, I., Jarvis, K.E., 1990. Rare earth element geochemistry of massive sulfides-sulfates and gossans on the Southern Explorer Ridge. Geology 18, 583-586.

Bau, M., Dulski, P., 1999. Comparing yttrium and rare earths in hydrothermal fluids from the Mid-Atlantic Ridge: implications for Y and REE behavior during near-vent mixing and for the Y/Ho ratio of Proterozoic seawater. Chem. Geol. 155, 77-90.

Bender, M.L., Klinkhammer, G.P., Spencer, D.W., 1977. Manganese in sea water and the marine manganese balance. Deep Sea Res. 24, 799-812.

Biscaye, P.E., 1965. Mineralogy and sedimentation of recent deep-sea clays in the Atlantic Ocean and adjacent seas and oceans. Bull. Geol. Soc. Am. 76, 803-832.

Chamley, H., 1989. Clay sedimentology, Springer- Verlag, Berlin, pp. 623

Chavagnac V., German, C.R., Milton, J.A, Palmer M.R., 2005. Sources of REE in sediment cores from the rainbow vent site (36°14'N, MAR), Chem. Geol. 216, 329-352

Chernova, T.G., Rao, P.S., Pikovskii, Yu. I., Alekseeva, T.A., Nath, B.N., Rao, B.R., Rao. Ch.M., 2001. The composition and source of hydrocarbons in sediments taken from the tectonically active Andaman Backarc Basin, Indian Ocean. Mar. Chem. 75, 1-15.

Colin, C., Turpin, L., Bertaux, J., Desprairies A., Kissel, C. 1999. Erosional history of the Himalayan and Burman ranges during the last two glacial–interglacial cycles. Earth Planet. Sci. Lett. 171, 647-660.

Cronan, D.S., 1976. Basal metalliferous sediments from the eastern Pacific. Geol. Soc. of Am. Bull. 87, 928-934.

Cronan, D.S., Wijayananda, N.P., 1991. Sediments and marine mineral resources in the eastern Indian Ocean. Mar. Mining, 10, 103-116.

Curray J.R., 2005. Tectonics and history of the Andaman Sea region. Jr. Asian Earth Sci. 25, 187–232.

Curray, J.R., Moore, D.G., Lawver, L.A., Emmel, F.J., Raitt, R.W., Henry, M., Kieckhefer, R., 1979. Tectonics of the Andaman Sea and Burma. In: Watkins, J., Montadert, L., Dickerson, P.W. (Eds.), Geological and Geophysical Investigations of Continental Margins American Association Petroleum Geologists Memoir 29, pp. 189–198.

Dymond, J., Corliss, J. B., Heath, G.R., Filed, C.W., Dasch, E.J., Veeh, H.H., 1973. Origin of metalliferous sediments from the Pacific Ocean. Geol. Soc. Am. Bull. 8, 3355-3371.

El Wakeel S.K., Riley J.P., 1957. Determination of organic matter in marine muds. J. Conseil Int. Explor. Mer. 22, 180-183.

Elderfield, H., 1988. The oceanic chemistry of the rare earth elements. Phil. Trans. R. Soc. London A 325, 105-126.

Elderfield, H., Greaves, M.J., 1981. Negative cerium anomalies in the rare earth element patterns of oceanic ferromanganese nodules. Earth Planet. Sci. Lett. 55, 163-170.

Folk, R.L, 1968. Petrology of sedimentary rocks, Hemphills, Austin, Texas, pp.170.

Froelich, P.N., Klinkhammer G.P., Bender, M. L., Luedtke, N.A., Heath, G.R., Cullen, D., Dauphin. P., 1979. Early oxidation of organic matter in pelagic sediments of the eastern equatorial Atlantic: suboxic diagenesis. Geochim. Cosmochim. Acta, 43, 1075-1090.

German, C.R., Hergt, J., Palmer, M.R., Edmond, J.M., 1999. Geochemistry of a hydrothermal sediments core from the OBS vent-field, 21°N East Pacific Rise. Chem. Geol. 155, 65-75.

German, C.R., Mills, R., Blusztajn. J., Fleer, A.P., Bacon, M.P., Higgs, N.C., Elderfield, H., Thomson, J., 1993. A geochemical study of metalliferous sediment from the TAG hydrothermal mound, 26°08'N, Mid Atlantic Ridge. J. Geophys. Res. 98, 9683-9692.

Glasby, G.P., Gwozdz, R., Kunzendorf, H., Friedrich, G., Thijssen, T., 1987. The distribution of rare earth and minor elements in manganese nodules and sediments from the equatorial and S.W. Pacific. Lithos. 20, 97-113.

Hathon, E.G., Underwood, M.B., 1991. Clay mineralogy and chemistry as indicators of hemipelagic sediment dispersal south of the Aleutian arc. Mar. Geol. 97, 145-166.

Hodkinson R.A, Varnavas, S., Perissoratis., C., 1994. Regional geochemistry of sediments from the Hellenic Volcanic Arc in regard to submarine hydrothermal activity. Mar. Georesource. Geotech. 12, 83-129.

Kamesh Raju, K.A., Ramprasad, T., Rao, P.S., Rao, B.R., Varghese, J., 2004. New insights into the tectonic evolution of the Andaman basin, northeast Indian Ocean. Earth Planet. Sci. Lett. 221, 145-162.

Konta, J., 1985. Mineralogy and chemical maturity of suspended matter in major river samples under the SCOPE/UNEP project. In: Transport of carbon and minerals in major world rivers, Part 3, (Eds). E. T. Degens and S. Kempe, Vol. 58, pp. 559-568, Mittilungen aus dem Geologisch-Palaeontologischen, Institut der Universitat Hamburg

McLennan S.M., 1989. Rare earth elements in sedimentary rocks: Influence of provenance and sedimentary processes. In: B.P. Lipin & G.A. Mckay (Editors) Geochemistry and Mineralogy of Rare earth elements. Rev. in Mineralogy. 21. 116-200.

Michard, A., Albarède, F., Michard, G., Minster, J.F., Charlou J.L., 1983. Rare earth elements and uranium in high temperature solutions from East Pacific Rise hydrothermal vent field (13°N). Nature, 303, 795-797.

Mills, R., Elderfield, H., Thomson, J., 1993. A dual origin for the Hydrothermal component in a metalliferous sediment core from the Mid-Atlantic Ridge. J. Geophys. Res. 98 (B6), 9671-9681.

Nath, B.N., Balaram, V., Sudhakar, M., Pluger, W.L., 1992. Rare earth element geochemistry of ferromanganese deposits of the Indian Ocean. Mar. Chem., 38, 185-208.

Nath, B.N., Bau, M., Rao, B.R., Rao, Ch. M., 1997. Trace and rare earth elemental variation in Arabian Sea sediments through a transect across the oxygen minimum zone. Geochim. Cosmochim. Acta 61, 2375-2388.

Nath, B.N., Kunzendorf, H., Pluger, W.L., 2000. Influence of provenance, weathering and sedimentary processes on the elemental ratios of the fine-grained fraction of the bedload sediments from the Vembanad Lake and the adjoining continental shelf, southwest coast of India. J. Sed. Res. 70, 1081-1094.

Nath, B.N., Roelandts, I., Sudhakar, M., Plüger, W.L., Balaram, V., 1994. Cerium anomaly variations in ferromanganese nodules and crusts from the Indian Ocean. Mar. Geol, 120, 385-400.

Palmer, M.R., 1985. Rare earth elements in foraminifera. Earth Planet. Sci. Lett, 186, 383-399.

Parra, M., Chapuy, B., Pons. J., Latouche, C., 1991. The nature and origin of smectites in the Kerguelen-Heard Archipelagoes of the southern Indian Ocean. Cont. Shelf Res. 11, 347-364.

Piper, D.Z., 1974. Rare earth elements in the sedimentary cycle: a summary. Chem. Geol. 14, 285-304.

Plank, T., Langmuir, C.H., 1998.The chemical composition of subducting sediment and its consequences for the crust and mantle. Chem. Geol. 145, 325-394.

Ramaswamy, V., Gaye, B., 2006. Regional variations in the fluxes of foraminifera carbonate, coccolithophorid carbonate and biogenic opal in the northern Indian Ocean. Deep Sea Res. 53, 271-293.

Ramaswamy, V., Rao, P.S., Rao, K.H., Thwin, S., Rao, N.S., Raiker, V., 2004. Tidal influence on suspended sediment distribution and dispersal in the northern Andaman Sea and Gulf of Martaban. Mar. Geol. 208, 33–42.

Rao P.S., Ramaswamy, V., Thwin, S., 2005. Sediment texture, distribution and transport on the Ayeyarwady continental shelf, Andaman Sea. Mar. Geol. 216, 239-247.

Rao, P.S., Kamesh Raju, K.A., Ramprasad, T., Nath, B.N., Rao, B.R., Rao. Ch.M., Nair, R.R., 1996. Evidence for hydrothermal activity in the Andaman Backarc Basin. Curr. Sci. 70, 379-385.

Reitz, A., Thomson, J., De Lange, G.J., Hensen, C., 2006. Source and development of large manganese enrichments above eastern Mediterranean sapropel S1. Paleoceanography, 21, PA3007, doi:10.1029/2005PA001169.

Rodolfo, K.S., 1969. Sediments of the Andaman basin, North Eastern Indian Ocean. Mar. Geol. 7, 371-402.

Rodolfo, K.S., 1969a. Bathymetry and marine geology of the Andaman basin, and tectonic implications for South East Asia. Geol. Soc. Am. Bull. 80, 1203-1230.

Rona, P.A., Scott, D., 1993. A special issue on sea-floor hydrothermal mineralization New perspectives- Preface. Economic. Geol. 88, 1935- 1975

Roonwal, G.S., Glasby, G.P., Roelandts, I., 1997. Mineralogy and geochemistry of surface sediments from the Andaman Sea and upper Nicobar Fan, northeast Indian Ocean. Jr. Ind. Ass. Sedimentologist 16, 89-101.

Rutten, A., De Lange, G.J., 2003. Sequential extraction of iron, manganese and related elements in S1 sapropel sediment, eastern Mediterranean. Paleogeogr., Paleoclimatol., Paleoecol, 190, 79-101.

Schaller, T., Morford, J., Emerson, S. R., Feely, R.A., 2000. Oxyanions in metalliferous sediments: Tracers for paleoseawater metal concentrations? Geochim. Cosmochim. Acta. 63, 2243-2254.

Sholkovitz, E.R., 1990. Rare earth elements in marine sediments and geochemical standards. Chem. Geol. 88, 333-347.

Siby, V., 2004. Geochemistry of rare earth elements and trace metals along the western continental shelf of India. Ph.D thesis, Cochin University of Science and Technology, Kerala (unpublished), pp.238.

Sirocko, F., Garbe-Schönberg D., Devey C., 2000. Processes controlling trace element geochemistry of Arabian Sea sediments during the last 25,000 years**.** Global Planet. Change,26, 217-303.

Stoll, H. M., Arevalos, A., Burke, A., Ziveri, P., Mortyn, G., Shimizu, N., Unger, D., 2007. Seasonal cycles in biogenic production and export in northern Bay of Bengal sediment traps. Deep Sea Res. II, doi:10.1016/j.dsr2.2007.01.002.

Stow, D.A.V., 1985. Fine grained sediments in deep water: an overview of processes and facies models. Geo. Mar. Letts. 5, 17-23.

Taylor, S.R., McLennan, S.M., 1985. The continental crust: its composition and evolution Blackwell Scientific Publications, Oxford. pp. 312.

Thomson, J., Higgs, N. C., Wilson, R. R. S., Croudace, I. W., de Lange, G. J., van Santvoort, P. J. M., 1995. Redistribution and geochemical behaviour of redox-sensitive elements around S1, the most recent eastern Mediterranean sapropel, Geochim. Cosmochim. Acta, 59, 3487- 3501.

Venkatesan, M.I., Ruth, E., Rao, P. S., Nath , B.N., Rao, B.R., 2003. Hydrothermal petroleum in the sediments of the Andaman Backarc Basin, Indian Ocean. App. Geochemistry. 18, 845-861.

Wyrtki, K., 1973. Physical oceanography of the Indian Ocean. In: Zeitschel, B., Gerlach, S.A. (Eds.), The Biology of the Indian Ocean. Springer Verlag, Berlin, pp. 18– 36.

List of Figures

Table 1. Concentration of bulk and clay minerals in the sediment cores from the ABB

	Bulk minerals (%)		Clay minerals (%)				
Depth (cm)	Quartz	Plagioclase	Smectite	Illite	Chlorite	Kaolinite	K/Ch
SPC-1							
0-2	31.41	10.24	51.9	21.2	10	12.3	1.23
4-6	31.34	10.8	25.5	35.5	12.2	15.6	1.28
8-10	35.69	8.98	48.4	26.4	8.4	11.8	1.40
12-14	35.25	8.51	47.9	24.8	8.6	12.4	1.44
22-24	37.88	7	55.1	20.3	9	12.6	1.40
SPC- 2							
0-2	33.45	11.12	53.4	19.3	8.5	11.2	1.32
4-6	30.18	7.08	56.8	19.7	9.4	11.5	1.22
8-10	28.46	7.44	59.9	19.4	7.4	10.2	1.38
16-18	28.34	5.82	55.5	22.1	7.5	10.7	1.43
SPC- 5							
0-2	28.8	9.65	55.2	19.5	10.2	11.3	1.11
2-4	34.53	9.07	48.8	26	7.2	13.3	1.85
10-12	35.17	8.49	59.9	18.9	8.9	9.7	1.09
14-16	39.83	7.81	34.1	33.2	11.6	16.4	1.41
22-24	33.42	5.58	58.6	20.2	8.4	9.4	1.12
24-26	34.92	8.21	56.7	29	6.4	7.3	1.14

Table 2. Elemental concentration of Andaman backarc basin sediments and the surface sediments from the Irrawaddy shelf.

Depth (cm) SPC-1	$CaCO_3$	C_{org}	Al	Fe	Mn	K*	Ba*	Cr	Co	Ni	Cu	Zn	Y	Pb	Mo	Y/Ho
0-2	0.51	0.44	8.51	4.71	3.48	1.86	1295	105	29	177	82	89	35	90	44.1	54.4
2-4	0.30	1.26	8.30	4.34	4.07	1.91	1221	93	26	148	70	63	31	76	36.2	54.6
4-6	0.52	1.45	8.24	4.30	2.44	1.92	1165	94	27	136	69	68	31	82	12.1	52.6
6-8	1.85	1.31	8.07	4.47	1.97	1.93	1180	98	29	143	74	72	32	90	7.8	52.8
8-10	3.05	1.41	8.78	4.82	1.68	1.90	1150	107	31	146	76	76	34	90	6.2	53.9
10-12	3.27	1.28	8.65	4.75	1.46	1.94	1126	109	35	140	71	76	35	90	4.7	53.6
12-14	4.33	1.35	8.21	4.92	0.32	1.99	1023	104	21	100	100	59	34	92	1.6	51.9
14-16	4.97	1.31	8.27	4.85	0.09	1.98	968	100	17	96	57	91	34	90	0.9	54.2
16-18	4.84	1.39	8.03	4.76	0.07	1.95	870	97	16	93	56	86	31	93	0.7	53.0
18-20	5.38	1.96	8.49	4.88	0.07	2.03	811	106	16	106	74	71	33	70	0.7	53.1
20-22	5.33	1.64	8.11	4.49	0.06	2.04	805	95	15	84	47	95	28	51	0.6	52.9
22-24	6.66	1.26	8.70	5.05	0.07	2.01	792	108	17	95	47	94	32	49	0.5	53.3
24-26	7.93	1.86	8.29	4.37	0.07	2.04	667	93	15	85	42	73	27	46	0.6	53.0
26-28	5.89	1.35	8.26	4.46	0.08	-	-	96	16	81	33	46	26	35	0.8	51.5
SPC-2																
0-2	2.08	1.82	8.59	4.52	1.97	N.A	N.A	99	31	138	77	66	29	74	16.2	54.2
2-4	4.58	1.79	8.88	4.55	1.23	-	-	102	29	129	70	73	32	78	5.7	54.1
4-6	8.92	1.74	8.84	4.54	1.06	-	-	101	30	131	66	73	31	74	3.0	52.5
6-8	11.25	1.77	8.81	4.47	0.61	-	-	97	23	125	61	63	28	61	1.5	53.5
8-10	14.08	1.40	9.06	4.58	0.39	-	-	99	24	127	53	64	31	55	1.0	52.9
10-12	14.17	1.65	8.63	4.23	0.24	-	-	88	20	115	52	70	28	38	0.6	53.7
12-14	17.42	1.56	8.56	3.81	0.33	-	-	86	22	120	48	69	27	31	0.6	53.9
14-16	18.50	1.66	8.87	3.70	0.41	-	-	86	24	123	43	56	27	37	0.6	54.1
16-18	17.92	1.65	8.96	3.66	0.44	-	-	88	24	125	42	66	27	33	0.5	54.3
SPC-5																
0-2	2.77	1.61	8.65	4.52	2.12	1.78	1232	105	29	153	68	79	33	64	10.5	54.0
2-4	4.99	1.72	8.87	4.46	1.57	1.83	1164	105	29	152	67	79	33	66	6.5	54.3
10-12	3.95	1.35	8.93	4.94	2.01	1.92	1057	110	39	187	69	98	34	75	9.4	54.8
14-16	5.46	1.38	8.40	5.32	0.10	1.95	896	104	19	125	67	93	34	100	0.9	53.3
22-24	6.82	1.53	8.78	4.59	0.09	2.04	777	105	19	115	54	84	33	71	0.6	53.6
24-26	6.93	1.52	8.86	4.62	0.09	2.04	718	104	19	112	52	79	32	70	0.6	52.9
Irrawaddy																
40	1.50	0.85	8.74	6.07	0.12	N.A.	N.A.	171	26	153	33	83	30	25	0.8	51.5
47	0.80	0.62	8.68	5.95	0.13	-	-	149	25	132	29	75	35	45	1.2	50.7
50	1.10	0.88	8.62	6.09	0.13	-	-	150	26	136	32	88	37	36	1.1	51.6

1) $CaCO_3$, C_{org}, Al, Fe, Mn, K are in wt (%) and trace elements in ppm; 2) Y/Ho is the molar ratio; 3) * XRF data; 4) N.A: Not analyzed

Table 3. Rare earth element concentration (ppm) in the sediment cores from the ABB and the surface sediments from the Irrawaddy shelf

Depth (cm) SPC-1	La	Ce	Pr	Nd	Sm	Eu	Gd	Tb	Dy	Ho	Er	Tm	Yb	Lu	Ce-anomaly	$(La/Yb)_n$	$(Eu/Sm)_n$
0-2	36.8	73.6	7.7	31.7	6.95	1.67	5.73	1.00	5.64	1.20	3.54	0.53	3.18	0.48	1.00	0.85	1.24
2-4	32.0	64.4	6.7	27.6	6.05	1.48	5.08	0.87	5.07	1.04	3.09	0.45	2.78	0.41	1.02	0.85	1.26
4-6	33.2	66.5	7.0	28.9	6.26	1.54	5.25	0.86	5.29	1.10	3.14	0.46	2.85	0.42	1.01	0.86	1.26
6-8	34.1	68.8	7.2	29.7	6.51	1.53	5.43	0.92	5.33	1.11	3.18	0.47	2.88	0.42	1.01	0.88	1.21
8-10	38.0	75.5	7.9	32.2	6.97	1.68	5.83	0.98	5.73	1.19	3.56	0.51	3.16	0.46	1.00	0.89	1.24
10-12	39.4	78.6	8.2	33.2	7.21	1.67	5.93	1.02	5.85	1.23	3.57	0.52	3.18	0.48	1.01	0.91	1.19
12-14	38.0	76.4	7.9	32.7	6.92	1.62	5.65	0.97	5.72	1.21	3.53	0.52	3.15	0.47	1.01	0.89	1.20
14-16	38.3	75.1	7.9	33.0	6.81	1.58	5.66	0.95	5.57	1.15	3.40	0.49	3.12	0.47	0.99	0.91	1.19
16-18	37.8	75.5	7.9	32.4	6.88	1.59	5.55	0.95	5.34	1.10	3.16	0.47	2.88	0.43	1.01	0.97	1.19
18-20	39.9	79.4	8.4	34.2	7.26	1.62	5.85	0.98	5.47	1.14	3.40	0.49	2.99	0.44	1.00	0.99	1.14
20-22	36.6	72.8	7.6	31.5	6.48	1.42	5.26	0.86	4.89	1.00	2.89	0.42	2.59	0.36	1.00	1.04	1.13
22-24	44.3	87.2	9.2	37.1	7.63	1.67	6.11	1.03	5.50	1.13	3.34	0.48	3.07	0.43	1.00	1.06	1.12
24-26	37.4	74.5	7.9	32.0	6.70	1.45	5.37	0.88	4.71	0.95	2.77	0.40	2.41	0.36	1.00	1.14	1.11
26-28	40.9	80.7	8.5	34.2	6.95	1.42	5.56	0.88	4.89	0.95	2.77	0.38	2.46	0.35	1.00	1.23	1.05
SPC-2																	
0-2)	30.6	61.9	6.7	27.4	5.89	1.42	4.79	0.86	4.98	1.01	2.95	0.44	2.45	0.38	1.00	0.92	1.24
2-4	33.1	67.1	7.1	29.2	6.20	1.50	5.01	0.88	5.25	1.09	3.16	0.45	2.77	0.43	1.01	0.88	1.24
4-6	33.2	67.4	7.0	29.4	6.22	1.47	4.99	0.89	5.19	1.11	3.16	0.48	2.76	0.43	1.02	0.89	1.21
6-8	30.2	61.2	6.5	27.0	5.73	1.40	4.66	0.84	4.68	0.98	2.84	0.42	2.48	0.38	1.01	0.90	1.26
8-10	33.1	66.9	7.0	29.1	6.08	1.46	4.94	0.89	5.08	1.07	3.11	0.45	2.59	0.40	1.02	0.94	1.24
10-12	29.6	59.6	6.2	25.6	5.37	1.27	4.35	0.80	4.65	0.95	2.76	0.42	2.45	0.37	1.01	0.89	1.21
12-14	29.6	60.0	6.3	25.4	5.36	1.28	4.47	0.78	4.52	0.92	2.72	0.41	2.37	0.37	1.01	0.92	1.23
14-16	30.2	61.0	6.3	26.1	5.36	1.25	4.40	0.77	4.53	0.93	2.71	0.41	2.35	0.38	1.02	0.95	1.20
16-18	30.3	60.6	6.3	25.8	5.43	1.28	4.37	0.78	4.57	0.94	2.64	0.41	2.36	0.38	1.01	0.94	1.21
SPC-5																	
0-2	33.5	67.9	7.1	30.0	6.36	1.54	5.01	0.92	5.44	1.13	3.38	0.49	2.89	0.46	1.01	0.85	1.24
2-4	33.9	68.6	7.3	30.2	6.34	1.55	5.06	0.93	5.43	1.12	3.33	0.49	2.85	0.45	1.01	0.88	1.25
10-12	36.4	72.8	7.8	32.7	6.71	1.62	5.40	0.99	5.78	1.16	3.45	0.51	3.06	0.48	1.00	0.88	1.24
14-16	36.9	73.0	7.8	32.1	6.68	1.56	5.44	0.97	5.74	1.19	3.49	0.52	3.09	0.50	0.99	0.88	1.20
22-24	38.4	76.1	8.1	33.1	6.69	1.53	5.41	0.96	5.52	1.14	3.42	0.51	2.96	0.46	0.99	0.96	1.18
24-26	38.8	77.2	8.2	33.3	6.75	1.50	5.44	0.95	5.48	1.12	3.24	0.48	2.85	0.44	1.00	1.01	1.14
Irrawaddy (SK-175)																	
40	39.8	79.3	8.5	35.5	7.28	1.64	5.69	1.00	5.50	1.07	3.16	0.44	2.67	0.41	0.99	1.10	1.16
47	46.0	91.6	9.9	41.0	8.34	1.89	6.60	1.17	6.44	1.28	3.59	0.53	3.14	0.48	0.99	1.08	1.17
50	48.2	96.6	10.2	41.9	8.46	1.87	6.73	1.17	6.62	1.31	3.86	0.54	3.19	0.51	1.00	1.11	1.13

1) $(La/Yb)_n$ and $(Eu/Sm)_n$ are PAAS-normalized ratios

Table 4. Weight percent of elements soluble in chemically separable phases for the samples from the ABB.

Depth (cm)	Wt % leached	∑REE	Mn	Fe	Cr	Co	Ni	Cu	Zn	Pb	Sc	Ga	Rb	Y	Nb	Cs	Th
% Acetic acid soluble																	
SPC-1																	
0-2	15.6	5.21	2.99	0.54	2.56	0.15	7.00	7.20	11.28	2.28	2.58	0.41	0.54	8.20	0.01	0.26	0.29
4-6	19.6	4.62	3.45	1.37	10.85	0.19	8.63	6.53	4.91	0.35	1.72	0.45	0.27	7.22	0.01	0.02	0.24
8-10	15.0	7.58	-	1.87	2.10	0.21	11.04	5.58	7.79	0.86	1.57	0.39	0.59	11.49	0.01	0.05	0.79
12-14	14.3	10.06	-	2.70	2.46	0.51	11.58	5.58	3.51	1.21	2.43	0.36	0.46	14.93	0.02	0.08	0.56
22-24	16.0	11.88	-	3.25	2.37	5.65	8.50	7.72	3.48	26.46	1.73	0.31	0.59	17.10	0.02	0.02	0.60
SPC-2																	
0-2	14.8	6.64	3.08	0.45	3.06	0.13	5.50	4.44	5.47	0.60	1.67	0.35	0.44	9.88	0.01	0.01	0.59
4-6	14.8	12.14	7.19	0.75	2.70	0.32	7.56	3.57	4.20	0.39	1.48	0.41	0.49	17.14	0.01	0.03	1.11
8-10	23.6	14.56	22.00	0.64	2.39	1.13	6.38	1.32	-	5.05	2.49	0.63	0.83	19.00	0.03	0.05	1.70
16-18	27.9	20.52	57.94	0.89	2.16	7.06	9.94	2.75	1.74	15.62	2.19	1.55	1.45	26.19	0.23	0.11	1.25
SPC-5																	
0-2	13.4	7.20	3.43	0.38	1.37	0.12	8.27	3.43	2.30	0.32	1.63	0.36	0.35	10.51	0.01	0.00	0.47
2-4	15.4	10.70	4.93	0.66	1.72	0.25	10.67	3.86	5.86	0.81	2.45	0.51	0.63	15.14	0.01	0.06	1.16
10-12	16.7	9.76	4.45	0.49	1.04	0.32	18.95	4.11	4.59	0.26	1.47	0.60	0.59	13.75	0.01	0.03	0.57
14-16	16.8	11.52	20.51	1.47	1.42	2.84	8.53	2.94	0.45	18.07	1.67	0.38	0.69	15.63	0.00	0.04	0.68
22-24	15.3	11.53	-	1.41	0.93	4.36	7.38	2.48	-	24.78	1.42	0.31	0.50	15.59	0.01	0.00	0.81
24-26	13.8	14.50	-	2.45	1.16	5.91	8.84	2.92	0.39	17.48	1.53	0.33	0.44	19.74	0.16	0.01	1.15
%Hydroxylamine -HCl soluble																	
SPC-1																	
0-2	25.4	24.23	89.29	17.53	3.25	5.29	49.08	42.23	23.97	76.81	1.06	6.14	2.26	32.02	0.43	1.10	0.94
4-6	18.8	26.71	87.91	46.05	0.00	55.93	43.73	35.50	25.43	70.07	0.85	5.78	2.29	36.12	0.50	0.92	1.28
8-10	20.8	22.27	-	44.56	4.96	55.54	34.58	27.14	18.88	60.87	1.34	3.27	2.30	29.54	0.40	1.33	0.36
12-14	15.3	20.73	-	42.92	5.22	49.85	24.94	23.44	22.72	69.47	1.77	1.39	2.27	28.51	0.34	0.81	0.70
22-24	19.5	14.64	-	18.43	3.02	8.29	7.86	8.59	8.64	27.40	0.88	0.22	2.25	20.60	0.20	1.14	0.10
SPC-2																	
0-2	21.5	26.57	88.91	16.26	5.08	49.53	37.54	29.34	32.37	78.60	2.03	4.36	2.93	35.44	0.52	1.22	0.87
4-6	21.7	19.97	78.20	13.08	5.68	43.10	22.54	18.95	14.76	54.98	2.24	1.63	2.63	25.79	0.40	1.07	0.03
8-10	30.4	16.10	49.61	6.82	1.79	16.56	11.30	8.66	21.81	39.86	0.87	0.11	2.99	22.22	0.28	1.75	-
16-18	29.9	9.55	19.26	3.51	0.38	12.50	10.28	10.57	9.46	13.18	0.82	-	3.10	13.97	2.29	1.89	0.19
SPC- 5																	
0-2	20.6	26.06	94.45	14.80	5.58	56.48	43.86	30.40	22.11	94.08	2.22	4.27	2.60	35.15	0.46	1.06	0.74
2-4	20.1	17.68	77.40	11.84	4.51	46.88	30.16	20.41	24.61	67.32	2.59	1.25	2.38	24.21	0.36	1.41	0.03
10-12	23.0	17.95	74.39	11.49	3.22	56.27	29.79	23.11	28.79	63.79	2.94	3.55	2.32	24.48	0.45	1.13	0.51
14-16	31.9	17.50	25.17	26.97	2.95	10.91	11.56	20.94	24.42	75.92	2.08	0.33	2.81	25.74	0.31	1.41	-
22-24	21.0	15.19	-	14.07	3.29	11.61	11.82	19.58	13.11	49.29	0.92	0.12	2.59	22.34	0.30	0.83	-
24-26	18.0	8.97	-	13.45	2.01	8.06	8.17	9.89	11.35	18.03	0.60	-	1.99	13.67	5.16	0.84	-

% HCl soluble																	
SPC-1																	
0-2	38.4	31.20	6.01	60.51	44.44	86.74	34.13	43.99	51.02	13.57	24.76	30.48	15.38	29.36	2.18	18.92	16.03
4-6	33.3	32.43	6.89	0.00	44.60	36.67	38.35	51.73	48.72	26.29	27.91	32.16	16.10	29.71	2.29	18.63	17.49
8-10	33.6	33.08	-	0.00	47.56	37.63	43.73	57.80	54.62	16.42	28.47	31.88	16.56	31.34	2.44	20.74	18.56
12-14	31.5	32.64	-		47.23	42.14	50.68	64.05	55.59	26.14	28.52	32.19	16.27	29.98	1.95	18.71	20.03
22-24	32.7	32.10	-	0.00	47.21	71.62	63.83	48.23	50.01	38.17	35.08	31.03	17.51	30.86	0.90	21.30	34.49
SPC-2																	
0-2	36.7	36.37	6.74	64.86	50.65	44.50	48.09	62.81	53.28	19.25	29.94	34.32	18.82	33.52	3.63	22.02	18.15
4-6	35.6	34.47	12.31	66.91	46.43	48.65	54.93	63.53	51.20	9.99	28.89	32.31	17.75	32.15	2.07	19.79	20.44
8-10	43.6	36.46	25.64	75.59	53.68	72.15	63.09	48.13	47.79	20.22	35.83	33.10	20.24	34.88	1.46	23.91	24.25
16-18	46.1	33.39	19.44	75.18	50.99	67.59	59.28	48.16	62.26	-	37.65	32.53	19.43	33.03	12.24	24.22	34.53
SPC-5																	
0-2	34.3	29.16	-	62.77	46.06	36.24	37.96	59.31	38.53	-	24.77	30.48	15.24	26.32	2.18	17.30	13.85
2-4	34.4	35.86	15.93	67.51	49.39	46.39	49.08	61.10	47.61	3.94	27.22	34.38	17.83	34.14	2.45	18.75	17.67
10-12	37.1	38.00	19.60	68.43	50.25	38.42	43.51	67.89	54.09	33.62	26.81	32.84	17.13	37.06	2.81	20.38	15.46
14-16	35.3	33.76	46.75	-	50.67	74.97	66.29	50.14	66.08	2.15	28.09	32.00	16.71	32.13	0.92	19.20	19.56
22-24	34.5	35.94	-	-	50.09	71.51	65.18	49.91	62.32	19.47	32.52	32.03	17.92	35.20	0.91	20.29	24.17
24-26	30.1	39.45	-	0.00	49.99	71.27	63.77	45.99	60.15	12.32	33.45	30.36	18.45	39.12	24.22	20.92	27.00
%Detrital (HCl insoluble residue)																	
SPC-1																	
0-2	61.6	39.35	1.71	21.42	49.76	7.82	9.79	6.57	13.72	7.34	71.60	62.97	81.82	30.42	97.38	79.72	82.74
4-6	66.7	36.24	1.75	52.57	44.55	7.21	9.29	6.24	20.94	3.28	69.52	61.62	81.34	26.95	97.20	80.43	80.98
8-10	66.4	37.07	-	53.57	45.38	6.62	10.64	9.48	18.71	21.86	68.62	64.46	80.55	27.63	97.16	77.89	80.28
12-14	68.5	36.57	-	54.39	45.09	7.50	12.81	6.93	18.18	3.18	67.28	66.05	81.00	26.58	97.69	80.40	78.71
22-24	67.3	41.39	-	78.32	47.40	14.44	19.81	35.46	37.87	7.97	62.31	68.44	79.65	31.44	98.87	77.55	64.82
SPC-2																	
0-2	63.4	30.43	1.26	18.43	41.21	5.84	8.87	3.41	8.88	1.55	66.35	60.97	77.81	21.16	95.84	76.74	80.39
4-6	64.4	33.43	2.30	19.26	45.20	7.93	14.97	13.95	29.83	34.65	67.39	65.65	79.13	24.92	97.52	79.11	78.42
8-10	56.4	32.88	2.74	16.96	42.14	10.16	19.23	41.90	30.40	34.87	60.81	66.17	75.95	23.90	98.23	74.29	74.05
16-18	53.9	36.53	3.37	20.42	46.47	12.86	20.49	38.52	26.55	71.20	59.33	65.92	76.01	26.80	85.25	73.78	64.03
SPC-5																	
0-2	65.7	37.58	2.13	22.05	47.00	7.16	9.92	6.86	37.06	5.60	71.38	64.89	81.81	28.02	97.35	81.63	84.94
2-4	65.6	35.76	1.73	19.99	44.37	6.47	10.09	14.63	21.91	27.93	67.74	63.86	79.16	26.52	97.17	79.78	81.15
10-12	63.0	34.29	1.57	19.59	45.50	5.00	7.75	4.89	12.53	2.33	68.79	63.00	79.97	24.70	96.73	78.46	83.46
14-16	64.8	37.22	7.57	71.56	44.96	11.28	13.62	25.99	9.05	3.86	68.16	67.29	79.80	26.50	98.77	79.36	79.76
22-24	65.5	37.34	-	84.53	45.70	12.51	15.62	28.03	24.56	6.45	65.14	67.54	78.99	26.88	98.77	78.88	75.02
24-26	69.9	37.09	-	84.10	46.84	14.76	19.23	41.20	28.11	52.17	64.43	69.31	79.12	27.47	70.46	78.23	71.85

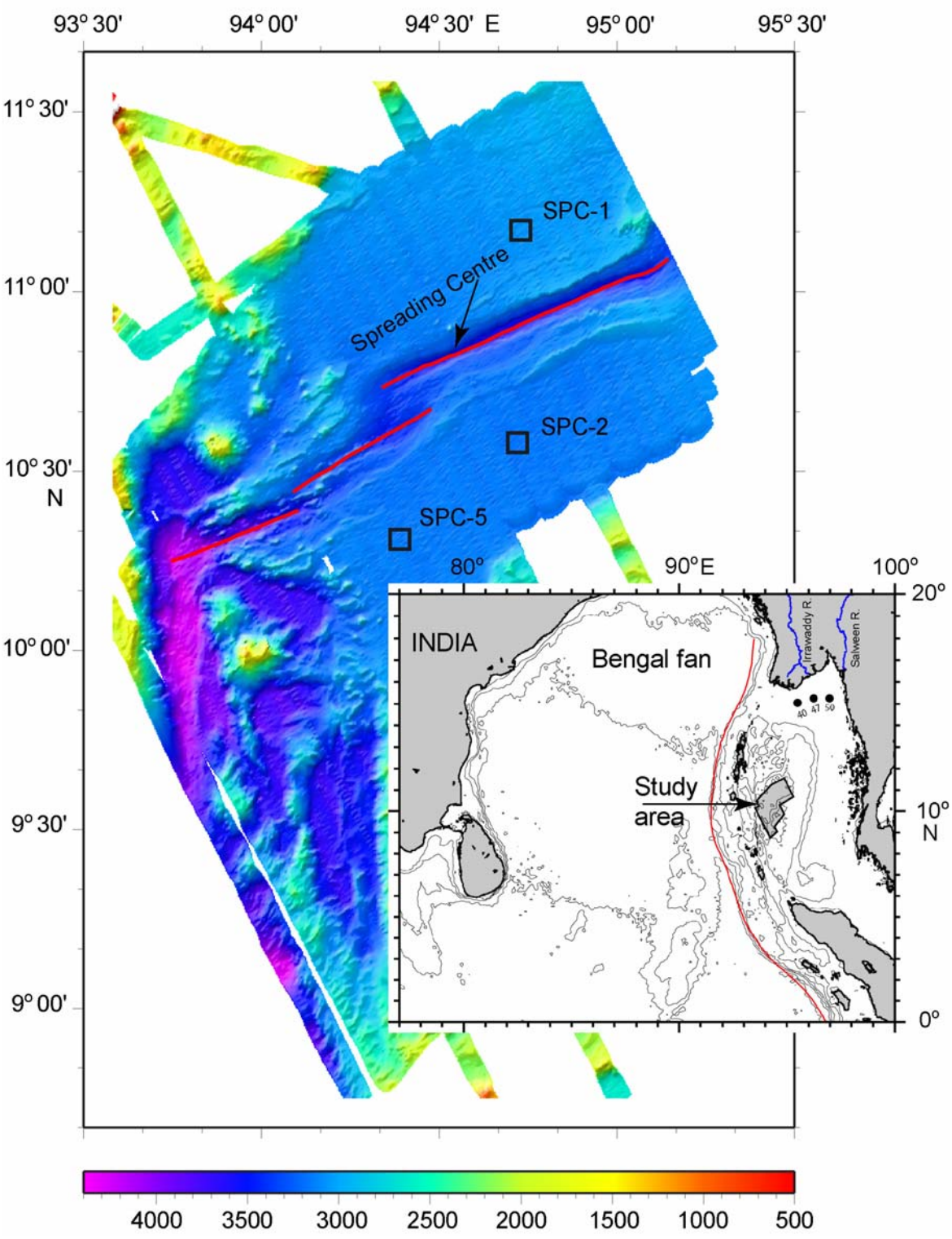

Kurian et al., Figure 1

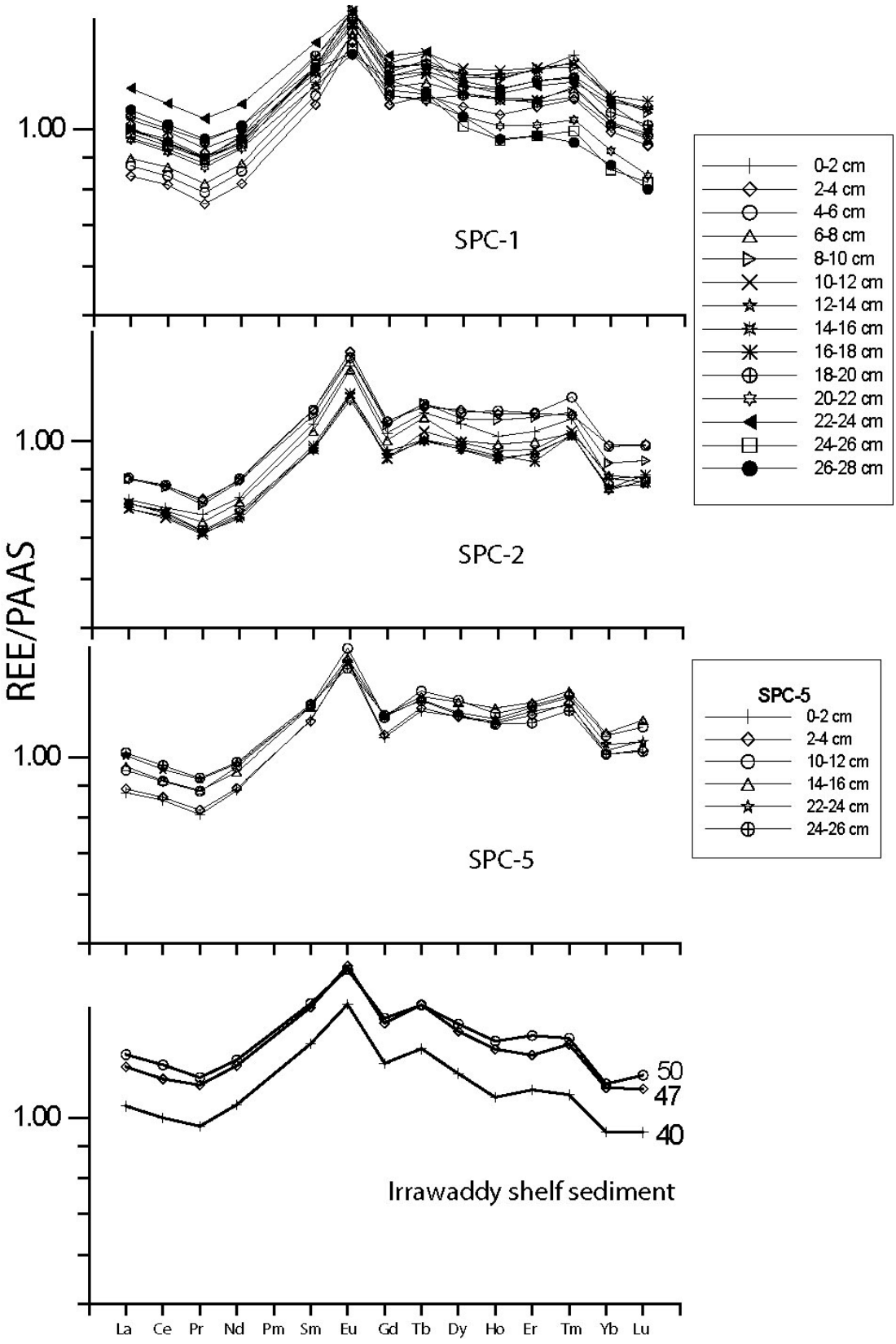

Kurian et al., Figure 2

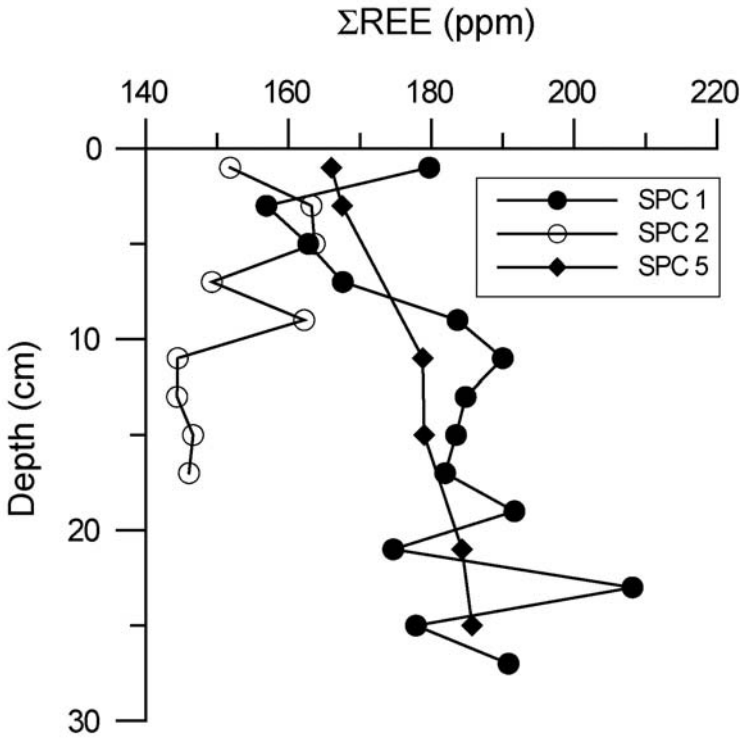

Kurian et al., Figure 3A

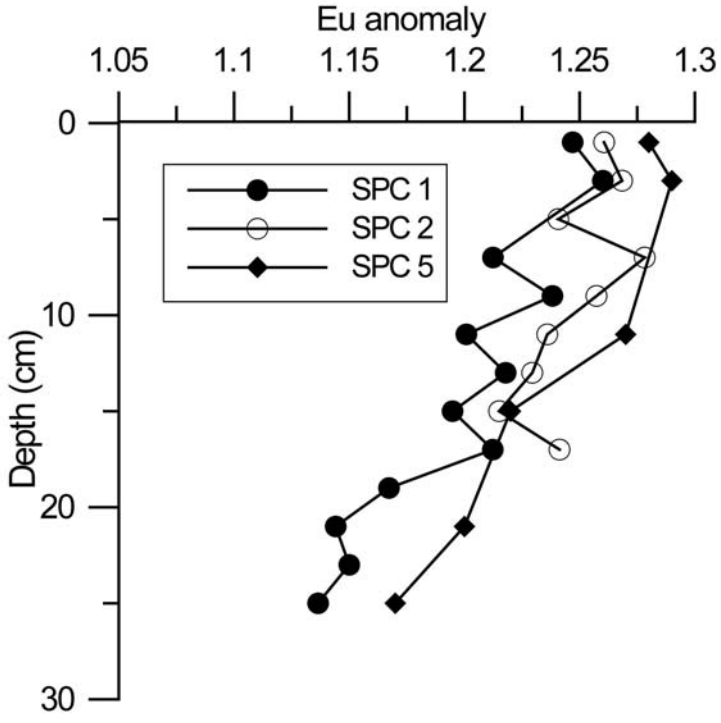

Kurian et al., Figure 3B

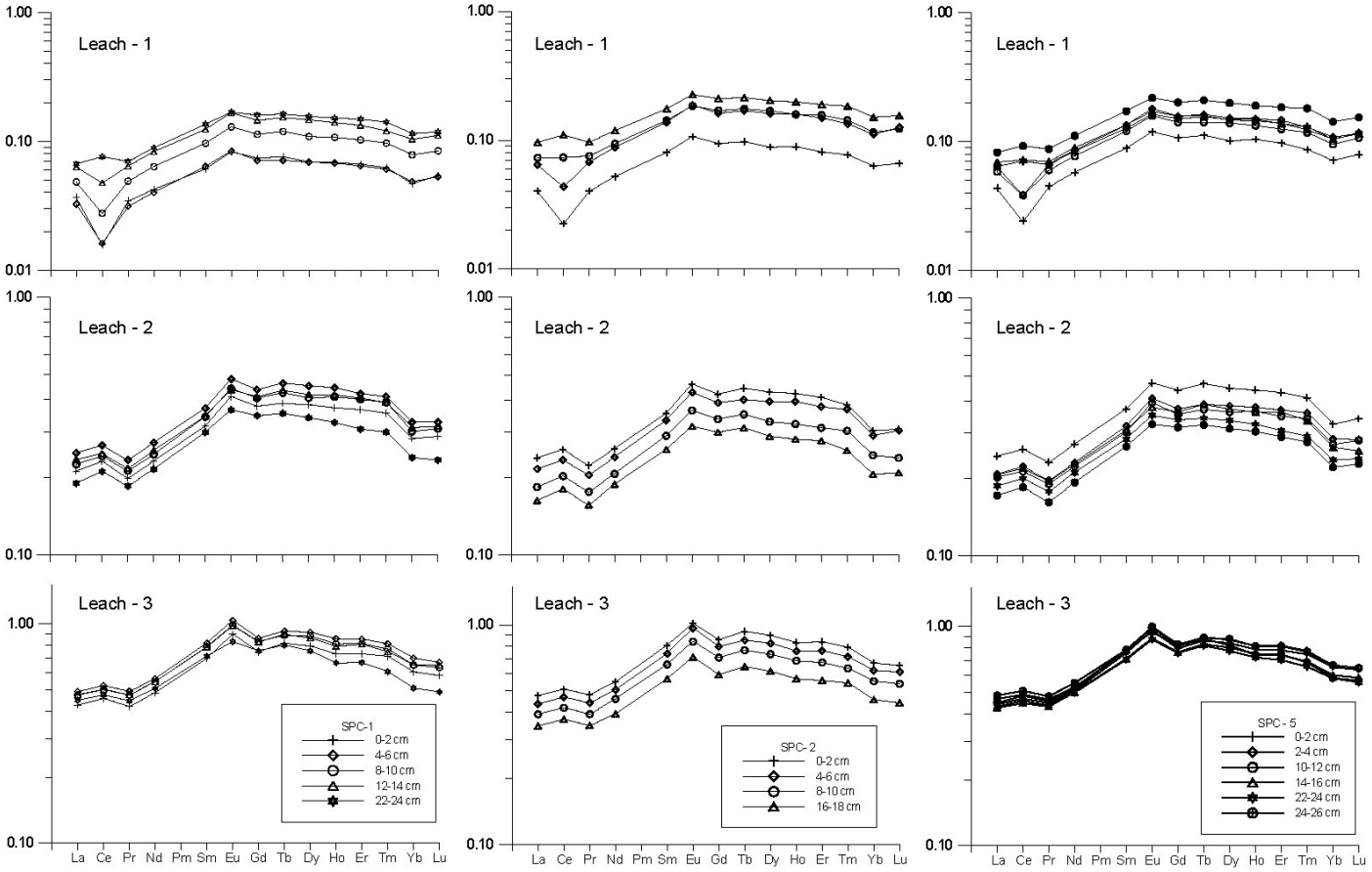

Kurian et al., Figure 4

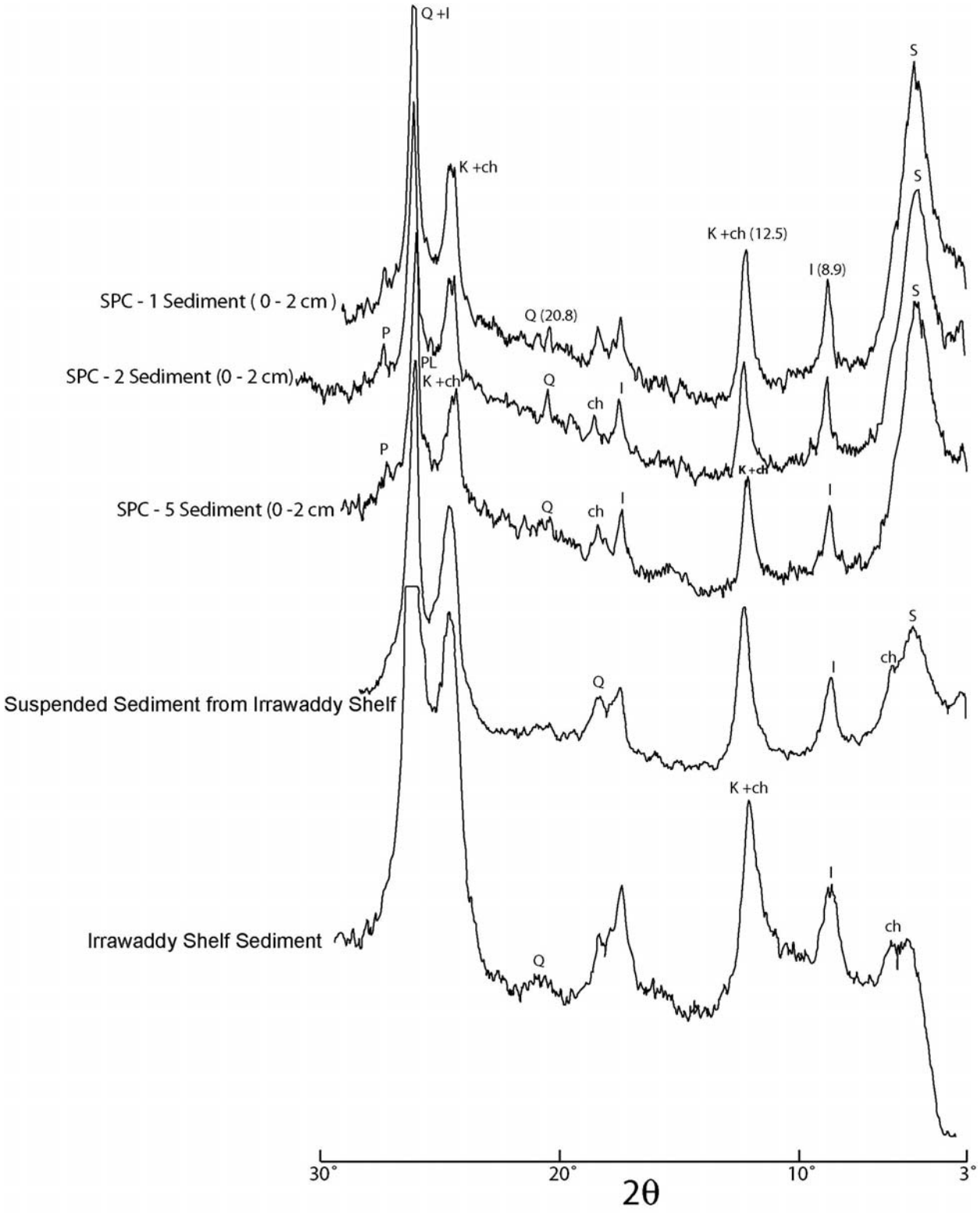

Kurian et al., Figure 5

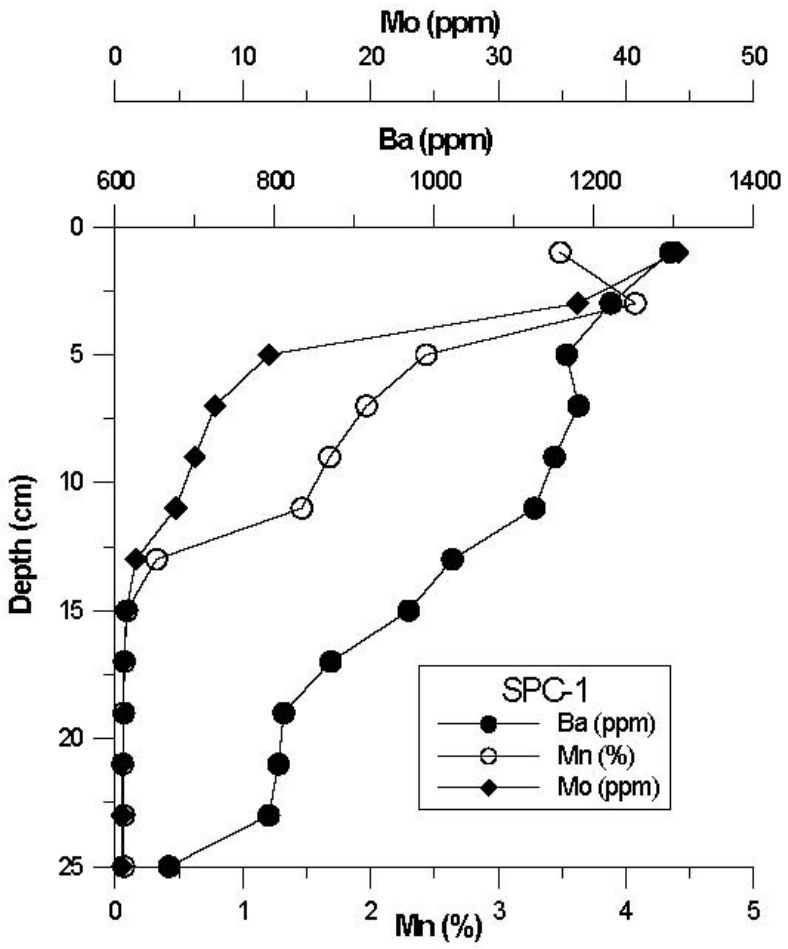

Kurian et al., Figure 6

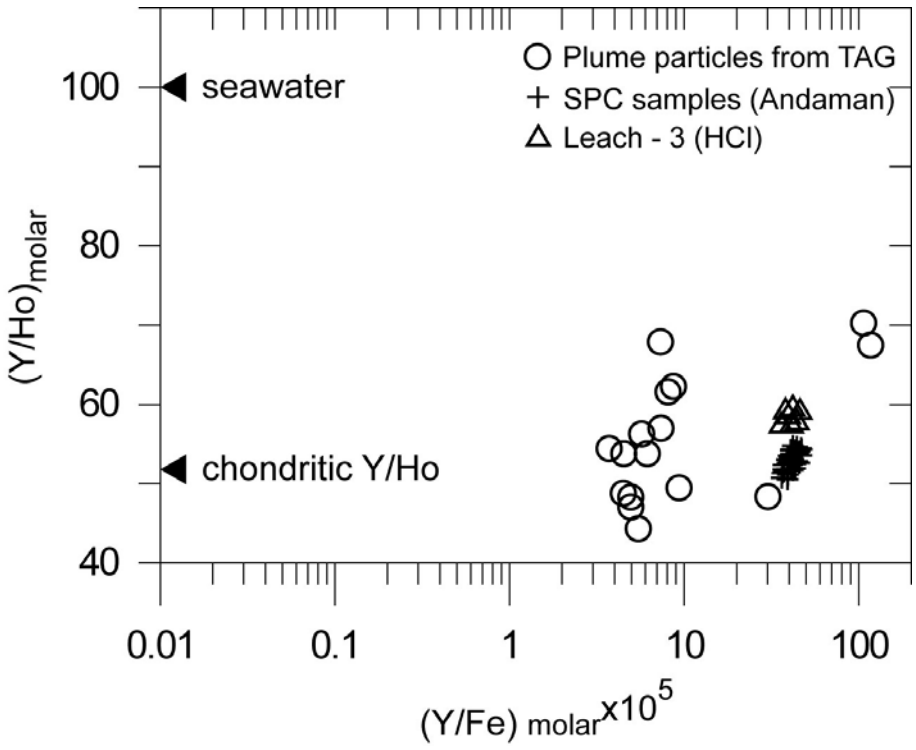

Kurian et al., Figure 7